Chinese Physics Letters

LETTER

The Heavy Flavor Conserving Hadronic Weak Decay of the Ground-State Bottom Baryons

Cite as: Peng-Yu Niu *et al*. 2026 *Chin. Phys. Lett.* **43** 070202

DOI CSTR

Recommended Articles

Two-Body Hadronic Weak Decays of Bottomed Hadrons
Ying Zhang, Guangzhao He, Quanxing Ye, Da-Cheng Yan, Jun Hua, and Qian Wang
Chin. Phys. Lett. **41**, (2024)

Status and Prospect of Weak Radiative Hyperon Decays
Rui-Xiang Shi, Zekun Jia, Li-Sheng Geng, Haiping Peng, Qiang Zhao, and Xiaorong Zhou
Chin. Phys. Lett. **42**, 032401 (2025)

Elliptic Flow Differences between Baryons and Anti-Baryons in Heavy-Ion Collisions Using SMASH Model
Shuai Zhou, and Shusu Shi
Chin. Phys. Lett. **42**, 021201 (2025)

Medium Modifications of Heavy-Flavor Jet Angularities in High-Energy Nuclear Collisions
Yao Li, Shi-Yong Chen, Wei-Xi Kong, Sa Wang, and Ben-Wei Zhang
Chin. Phys. Lett. **42**, 011201 (2025)

Light Hadronic Decays of Spin-0 Partner of *X*(3872)
Hong-Shuo Gao, Zu-Xin Cai, Gang Li, and Shi-Dong Liu
Chin. Phys. Lett. **42**, 100201 (2025)

Experimental Advances on Light Baryon Spectroscopy at BESIII Experiment
Shi Wang, Hao Liu, Shuangshi Fang, and Xiongfei Wang
Chin. Phys. Lett. **43**, 050201 (2026)

A series journal of Chinese Physical Society distributed by IOP Publishing

iopscience.iop.org/cpl | cpl.iphy.ac.cn

Chinese Physics Letters

Chin. Phys. Lett. **43** 070202 (2026)

LETTER

DOI: 10.1088/0256-307X/43/7/070202
CSTR: 32039.14.0256-307X.43.7.070202

The Heavy Flavor Conserving Hadronic Weak Decay of the Ground-State Bottom Baryons

Peng-Yu Niu(牛鹏宇)[1,2,*], Qian Wang(王倩)[1,2,3,*], and Qiang Zhao(赵强)[4,5,6,*]

[1]Guangdong Provincial Key Laboratory of Nuclear Science, Institute of Quantum Matter, South China Normal University, Guangzhou 510006, China
[2]Guangdong-Hong Kong Joint Laboratory of Quantum Matter, Southern Nuclear Science Computing Center, South China Normal University, Guangzhou 510006, China
[3]Southern Center for Nuclear-Science Theory (SCNT), Institute of Modern Physics, Chinese Academy of Sciences, Huizhou 516000, China
[4]Institute of High Energy Physics, Chinese Academy of Sciences, Beijing 100049, China
[5]University of Chinese Academy of Sciences, Beijing 100049, China
[6]Center for High Energy Physics, Henan Academy of Sciences, Zhengzhou 450046, China

*Corresponding authors. Email: niupy@m.scnu.edu.cn; qianwang@m.scnu.edu.cn; zhaoq@ihep.ac.cn

In this work, the heavy-flavor-conserving (HFC) hadronic weak decays of bottom baryons are studied in the framework of the nonrelativistic constituent quark model (NRCQM). We show that the pole terms play an indispensable role in the description of the branching ratio of $\Xi_b^- \to \Lambda_b^0 \pi^-$. With the pole terms included, we can make reliable predictions for $\Xi_b^0 \to \Lambda_b^0 \pi^0$. A combined study of the HFC hadronic weak decays allows us to make a reasonable prediction for $\Omega_b^- \to \Xi_b^{-(0)} \pi^{0(-)}$, which can be searched for at the LHCb and Belle-II experiments.

Introduction

For the hadronic weak decay of heavy flavor baryons, the heavy quark is usually involved in the weak interaction. However, there is a special hadronic weak decay process, i.e., the heavy-flavor-conserving (HFC) hadronic weak decay, where the heavy flavor is conserved, such as $\Xi_c \to \Lambda_c \pi$ in the charm sector, and $\Xi_b \to \Lambda_b^0 \pi$, $\Omega_b \to \Xi_b \pi$ in the bottom sector. These processes, though limited by the phase space, have provided a unique way for probing the hadron structure and the transition mechanism in the non-perturbative QCD (non-pQCD) region.

As pointed out in Refs. [1–4], the charm quark will not only behave as a spectator, but also be involved in the weak interaction via $cs \to cd$. More specifically, when the pole terms induced by the $cs \to cd$ conversion are almost on-shell, they will largely enhance the transition amplitude. For instance, the intermediate Σ_c pole-term contribution is the key to understanding the experimental data for $\Xi_c \to \Lambda_c \pi$ [3]. In contrast, the bottom quark in the bottom baryon hadronic weak decays will behave only as a spectator. As a result, in the heavy quark limit, both the light degree of freedom and total angular momentum should be conserved, individually. Thus, the $\Xi_b \to \Lambda_b^0 \pi$ process is an S-wave decay, which is a parity-violating process, with the leading order transition operators in the heavy quark limit.

The interesting HFC hadronic weak decay of heavy baryons was noticed for the first time in the 1990s and studied with various methods (see Refs. [2–13] and references therein). Unfortunately, it is hard to simultaneously describe all the experimental data well. In our previous work [3], we proposed that the pole terms are crucial for understanding the branching ratio of $\Xi_c^0 \to \Lambda_c \pi^-$. Meanwhile, our calculation favors the lower bound $(0.19 \pm 0.07)\%$ of the branching ratio $\mathrm{Br}(\Xi_b^- \to \Lambda_b^0 \pi^-)$ measured by the LHCb collaboration [14]. However, the follow-up measurements indicate a larger branching ratio.

The experimental measurement of the branching ratio largely depends on the ratio of the fragmentation fractions $f_{\Xi_b^-}$ and $f_{\Lambda_b^0}$, which reflect the fragmentation fractions of $b \to \Xi_b^-$ and $b \to \Lambda_b^0$, respectively. Based on the earliest measurement [14]

$$\frac{f_{\Xi_b^-}}{f_{\Lambda_b^0}} \mathrm{Br}(\Xi_b^- \to \Lambda_b^0 \pi^-) = (5.7 \pm 1.8^{+0.8}_{-0.9}) \times 10^{-4}, \tag{1}$$

and the assumption that $f_{\Xi_b^-}/f_{\Lambda_b^0}$ is bounded between 0.1 and 0.3, which is estimated with the measurement of the production rates of other strange particles relative to their nonstrange counterparts [14], the $\mathrm{Br}(\Xi_b^- \to \Lambda_b^0 \pi^-)$ would lie in the range between $(0.57 \pm 0.21)\%$ and $(0.19 \pm 0.07)\%$.

Recently, the relative rate

$$\frac{f_{\Xi_b^-}}{f_{\Lambda_b^0}} \mathrm{Br}(\Xi_b^- \to \Lambda_b^0 \pi^-) = (7.3 \pm 0.8 \pm 0.6) \times 10^{-4}, \tag{2}$$

was updated with the proton-proton collision data at center-of-mass energy of $\sqrt{s} = 13$ TeV with an integrated luminosity of 5.5 fb^{-1} [15]. The center value is slightly larger than the old one. Benefiting from the independent measurement of $f_{\Xi_b^-}/f_{\Lambda_b^0}$ [16], a more accurate value of $\mathrm{Br}(\Xi_b^- \to \Lambda_b^0 \pi^-)$ is determined to be:

$$\mathrm{Br}(\Xi_b^- \to \Lambda_b^0 \pi^-) = (0.89 \pm 0.10 \pm 0.07 \pm 0.29)\%. \tag{3}$$

The last uncertainty is due to the SU(3) flavor symmetry assumption in the determination of $f_{\Xi_b^-}/f_{\Lambda_b^0}$. Compared with the previous measurement results, the uncertainty of the range of $\mathrm{Br}(\Xi_b^- \to \Lambda_b^0 \pi^-)$ has significantly decreased. It provides a strict limit to the phenomenological study for the HFC hadronic weak decay of bottom baryons.

In this work, we revisit the decay of $\Xi_b \to \Lambda_b^0 \pi$ in the framework of the non-relativistic constituent quark model (NRCQM), which can still provide quantitative descriptions of the transitions, although the model uncertainties of the NRCQM are unavoidable. In order to have a better constraint on the NRCQM parameters, we note that the mass of the constituent quarks has a recognized range of values. Relatively large uncertainties may arise from the coupling constants of the Hamiltonian, for instance, the spring constant varies in different models or in different flavor systems. In our previous work [3], a plausible range of the spring constant is taken, based on the studies of the baryon spectrum. Here, except for the mass of quarks, all the other parameter values are extracted from the experimental data of bottom baryon decay processes. Considering the lack of experimental data for the HFC hadronic weak decays of bottom baryons, the strong decays of Σ_b are involved to restrict the values of the parameters. Meanwhile, all the parameters will be compared with those extracted from the heavy baryon spectrum.

Received 9 April 2026; accepted 1 June 2026; published 7 July 2026

© 2026 Chinese Physical Society and IOP Publishing Ltd. All rights, including for text and data mining, AI training, and similar technologies, are reserved.

Check for updates

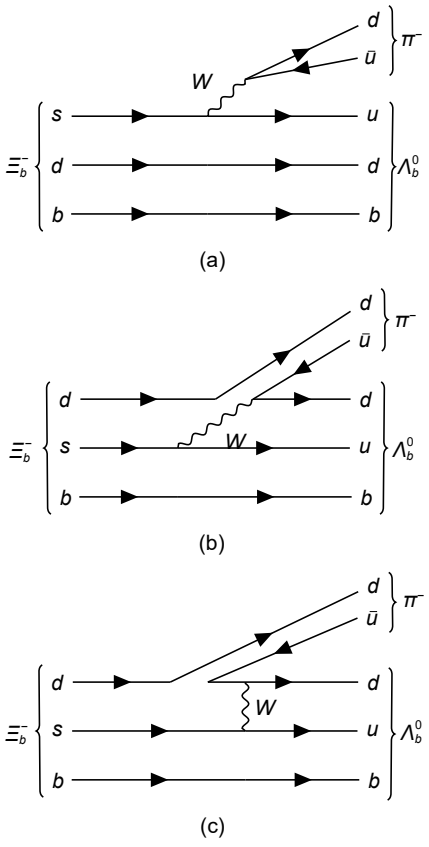

Fig. 1. The transition diagrams of the $\Xi_b^- \to \Lambda_b^0 \pi^-$. (a) DPE process; (b) CS-I process; (c) pole term.

Framework

The transition diagrams for the $\Xi_b \to \Lambda_b^0 \pi$ and $\Omega_b \to \Xi_b \pi$ processes are illustrated by Figs. 1–4. The hadronic weak decay of bottom baryons involves three kinds of processes. The first one is the direct pion emission (DPE) as shown in Fig. 1(a). The second one is the color-suppressed (CS) process that can be divided into two types. The first type describes the transition that the internal emitted W produces a new pair of quark and antiquark, which will immediately combine with one of the quarks of the initial baryons to form the final meson. We label it as type one of the color-suppressed process (CS-I) [Fig. 1(b)], while the second type of the color-suppressed process (CS-II) describes the transition that the constituent quarks of the final meson are all from the weak interaction vertex as shown in Fig. 2(b). The third typical transition is the pole term which can also be divided into two types. The first type is labeled as SW, where the meson is first produced by the strong interaction and then an intermediate state will propagate until two of the constituent quarks interact and convert into the final state hadron via the W exchange as shown in Fig. 1(c). The second type of the pole term, labeled as WS, describes the transition where the time order of the strong interaction and the weak interaction is reversed, as shown in Fig. 2(c). It should be stressed that the two transitions via Figs. 1(b) and 1(c) have totally different analytical structures and are dynamically different. To be more specific, figure 1(b) only contains the weak interaction and does not contain pole structures in its transition amplitude. In contrast, in Fig. 1(c), the strong and weak interactions are involved non-locally. The transition proceeds via two steps and has a pole structure in the transition amplitude that can manifest itself via experimental observables. This feature also makes it necessary to explicitly consider the pole terms in some of these weak decay transitions. As demonstrated in Refs. [3,4], the pole terms play an indispensable role in the HFC hadronic weak decays. As follows, we will present the wave functions and transition operators adopted in the calculation of the decay amplitudes.

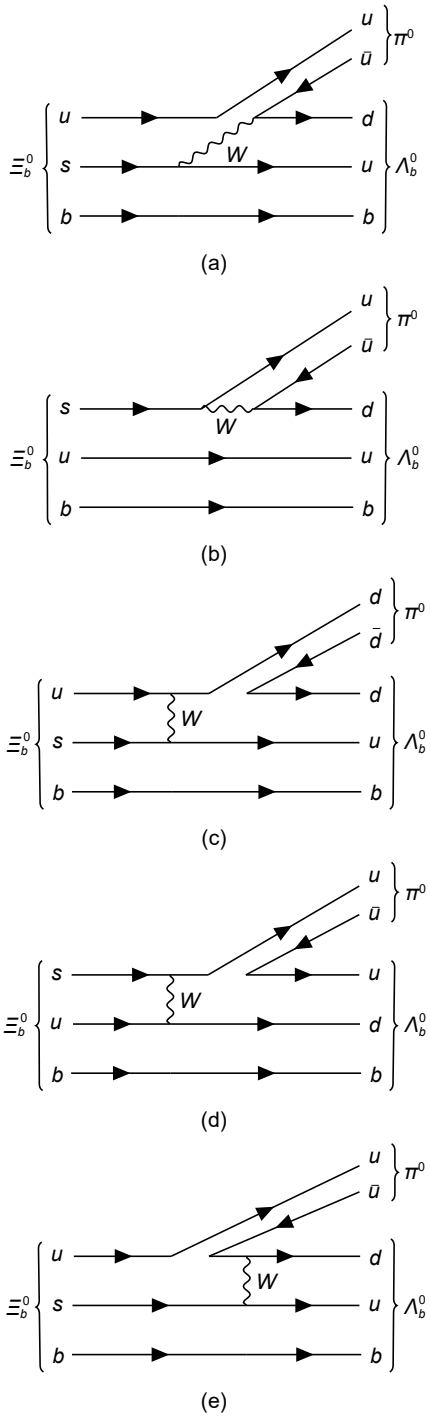

Fig. 2. The transition diagrams of the $\Xi_b^0 \to \Lambda_b^0 \pi^0$. (a) CS-I process; (b) CS-II process; (c) and (d) pole terms.

A. The Wave Function of Hadrons

In the framework of NRCQM, the hadron wave function is constructed with the color, flavor, spin, and spatial wave functions. Apart from the color wave function, the standard SU(6)⊗O(3) wave functions [17] are used in this work. The total wave functions for the bottom baryons and the pseudoscalar mesons can be found in Ref. [3]. For the wave function of the quark model, the main uncertainty stems from the spatial wave function. Technically, it is limited by the effective Hamiltonian for the quark and/or antiquark systems, which is insufficient for the description of the non-pQCD.

Generally, the effective Hamiltonian of the quark systems includes the kinetic energy, confinement potential, and short-range interaction or hyperfine interaction. Ignoring the hyperfine interaction

and taking the harmonic oscillator approximation, the effective Hamiltonian for the three-quark system [17,18] can be written as:

$$H=\sum_{i=1}^{3}\frac{\boldsymbol{p}_i^2}{2m_i^2}+\sum_{i\neq j}\frac{1}{2}K|\boldsymbol{r}_i-\boldsymbol{r}_j|^2\,, \tag{4}$$

where $\boldsymbol{r}_i$ and $\boldsymbol{p}_i$ are the coordinate and momentum for the ith quark. K is the spring constant that describes the strength of the interaction between quarks.

With the coordinate definitions

$$\boldsymbol{\rho}\equiv\frac{1}{\sqrt{2}}(\boldsymbol{r}_1-\boldsymbol{r}_2), \tag{5}$$

$$\boldsymbol{\lambda}\equiv\sqrt{\frac{2}{3}}\left(\frac{m_1}{m_1+m_2}\boldsymbol{r}_1+\frac{m_2}{m_1+m_2}\boldsymbol{r}_2-\boldsymbol{r}_3\right), \tag{6}$$

the corresponding momenta can be obtained as:

$$\boldsymbol{p}_\rho=m_\rho\dot{\boldsymbol{\rho}}=\sqrt{2}\left(\frac{m_2}{m_1+m_2}\boldsymbol{p}_1-\frac{m_1}{m_1+m_2}\boldsymbol{p}_2\right), \tag{7}$$

$$\boldsymbol{p}_\lambda=m_\lambda\dot{\boldsymbol{\lambda}}=\sqrt{\frac{3}{2}}\left(\frac{m_3}{M}\boldsymbol{p}_1+\frac{m_3}{M}\boldsymbol{p}_2-\frac{m_1+m_2}{M}\boldsymbol{p}_3\right). \tag{8}$$

As a result, the Hamiltonian can be expressed as:

$$H=\frac{\boldsymbol{P}^2}{2M}+\frac{\boldsymbol{p}_\rho^2}{2m_\rho}+\frac{\boldsymbol{p}_\lambda^2}{2m_\lambda}+\frac{1}{2}m_\rho\omega_\rho^2\boldsymbol{\rho}^2+\frac{1}{2}m_\lambda\omega_\lambda^2\boldsymbol{\lambda}^2\,, \tag{9}$$

where $\boldsymbol{P}$ is the total momentum of the baryon and $M=m_1+m_2+m_3$ is the total mass; m_ρ and m_λ are the reduced masses and defined as:

$$m_\rho=2\frac{m_1m_2}{m_1+m_2},\ m_\lambda=\frac{3}{2}\frac{m_3(m_1+m_2)}{M}. \tag{10}$$

Then, the spatial wave function, that is also referred to as the harmonic oscillator wave function, can be easily obtained and reads as

$$\Psi_{NLL_z}(\boldsymbol{P},\boldsymbol{p}_\rho,\boldsymbol{p}_\lambda)=\delta^3(\boldsymbol{P}-\boldsymbol{P}_c)\sum_m\langle l_\rho,m;l_\lambda,L_z-m|L,L_z\rangle \times\psi^{\alpha_\rho}_{n_\rho l_\rho m}(\boldsymbol{p}_\rho)\psi^{\alpha_\lambda}_{n_\lambda l_\lambda L_z-m}(\boldsymbol{p}_\lambda), \tag{11}$$

where

$$\psi^{\alpha}_{nlm}(\boldsymbol{p})=(i)^l(-1)^n\left[\frac{2n!}{(n+l+1/2)!}\right]^{\frac{1}{2}}\frac{1}{\alpha^{l+3/2}}\mathcal{Y}_{lm}(\boldsymbol{p}) \times L_n^{l+1/2}(\boldsymbol{p}^2/\alpha^2)\exp\left(-\frac{\boldsymbol{p}^2}{2\alpha^2}\right). \tag{12}$$

α_ρ and α_λ are the harmonic oscillator strengths that are determined by the reduced masses $m_{\rho/\lambda}$ and the frequencies $\omega_{\rho/\lambda}$:

$$\alpha_\rho^2=m_\rho\omega_\rho,\ \alpha_\lambda^2=m_\lambda\omega_\lambda, \tag{13}$$

with

$$\omega_\rho^2=\frac{3K}{m_\rho},\ \omega_\lambda^2=\frac{3K}{m_\lambda}. \tag{14}$$

When the hyperfine interaction is considered, the spatial wave function of the baryons can be expanded with the harmonic oscillator wave functions. Here, we still use the harmonic oscillator wave functions determined by Eq. (4). But the values of the harmonic oscillator strengths $\alpha_{\rho/\lambda}$ should be different from those that appear in the realistic spatial wave function. It can be understood that part of the effects from the hyperfine interaction are absorbed into $\alpha_{\rho/\lambda}$.

For the light mesons, as a quark-antiquark system, the spatial wave function of the ground state is expressed as:

$$\Psi(\boldsymbol{p}_1,\boldsymbol{p}_2)=\frac{1}{\pi^{3/4}R^{3/2}}\exp\left[-\frac{(\boldsymbol{p}_1-\boldsymbol{p}_2)^2}{8R^2}\right], \tag{15}$$

where R characterizes the size of mesons and is determined by the parameter K and the quark masses. For the pion, we take $R=0.28$ GeV, which is the same as in Ref. [3].

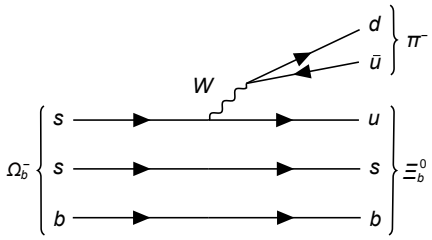

Fig. 3. The transition diagrams of the $\Omega_b^-\to\Xi_b^0\pi^-$. Only DPE process is allowed.

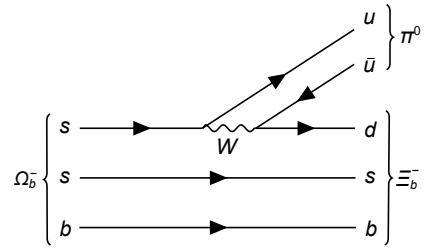

Fig. 4. The transition diagram of the $\Omega_b^-\to\Xi_b^-\pi^0$. Only CS-II process is allowed.

B. The Transition Operators

The Non-Relativistic Form of the Weak Interaction. The effective Hamiltonian that describes the four-fermion interaction is written as [17,19]:

$$H_{\rm W}=\frac{G_{\rm F}}{\sqrt{2}}\int{\rm d}\boldsymbol{x}\frac{1}{2}\{J^{-\mu}(\boldsymbol{x}),J^{+}_{\mu}(\boldsymbol{x})\}, \tag{16}$$

where

$$J^{+\mu}(\boldsymbol{x})=\begin{pmatrix}\bar{u} & \bar{c}\end{pmatrix}\gamma^\mu(1-\gamma_5)\begin{pmatrix}\cos\theta_{\rm C} & \sin\theta_{\rm C}\\ -\sin\theta_{\rm C} & \cos\theta_{\rm C}\end{pmatrix}\begin{pmatrix}d\\ s\end{pmatrix}, \tag{17}$$

$$J^{-\mu}(\boldsymbol{x})=\begin{pmatrix}\bar{d} & \bar{s}\end{pmatrix}\begin{pmatrix}\cos\theta_{\rm C} & -\sin\theta_{\rm C}\\ \sin\theta_{\rm C} & \cos\theta_{\rm C}\end{pmatrix}\gamma^\mu(1-\gamma_5)\begin{pmatrix}u\\ c\end{pmatrix}, \tag{18}$$

where $\theta_{\rm C}$ is the Cabibbo angle. The nonrelativistic form of the weak transition operators used in this work can be found in Ref. [3]. In this work, contributions from the QCD corrections will be absorbed into the quark model parameters, and the higher order processes such as the penguin diagrams [20] are neglected since their contributions are highly suppressed.

For the processes shown in Figs. 1(b), 2(a), 2(b), and 4, the color index of the d quark created by the weak interaction vertex is not arbitrary since the color indices of the other two quarks of the final baryon are fixed. Hence, these processes are color-suppressed and share the same color factor of $1/3$.

There exist the intermediate states in the pole terms. Only the contributions of ground states with $J^{\rm P}=1/2^+$ and the first excited bottom baryons with $J^{\rm P}=1/2^-$ are considered. All the possible states and their masses from different models are listed in Table 1. The values of masses used in our calculation are listed in the last line.

The Non-Relativistic Form of the Quark-Meson Interaction. We employ the chiral quark model [28–31] to describe the strong transition vertex. In this model, the pion couples to the light quark through a chiral Lagrangian for the pseudoscalar meson coupling to the constituent quark. At the leading order, the effective Hamiltonian reads as [28–31]:

$$H_\chi=\int{\rm d}\boldsymbol{x}\frac{g_{\rm A}^q}{f_{\rm m}}\bar{q}(\boldsymbol{x})\gamma_\mu\gamma_5 q(\boldsymbol{x})\partial^\mu\phi(\boldsymbol{x}), \tag{19}$$

where $q(\boldsymbol{x})$ is the light quark field. ϕ is the pseudoscalar octet and expressed as:

Table 1. The masses of the bottom baryons (MeV). Only their central values are listed. Here, we use the symbol $|^{(2s+1)}l_{\rm sym}\rangle$ to label the baryon state. l and s are the total orbital angular momentum and the total spin, respectively. The subscript "sym" is used to label the symmetry property of the corresponding spatial wave functions. The λ and ρ modes denote that the spatial wave function is symmetric or asymmetric under the interchange of the coordinate indices of the first two quarks, respectively. "$\cdots$" means that the data are unavailable from the corresponding references.

States	Ξ_b				Ξ'_b				Σ_b				Λ_b			
	$\|^2S\rangle$	$\|^2P_\lambda\rangle$	$\|^2P_\rho\rangle$	$\|^4P_\rho\rangle$	$\|^2S\rangle$	$\|^2P_\lambda\rangle$	$\|^2P_\rho\rangle$	$\|^4P_\lambda\rangle$	$\|^2S\rangle$	$\|^2P_\lambda\rangle$	$\|^2P_\rho\rangle$	$\|^4P_\lambda\rangle$	$\|^2S\rangle$	$\|^2P_\lambda\rangle$	$\|^2P_\rho\rangle$	$\|^4P_\rho\rangle$
PDG [21]	5792	$\cdots$	$\cdots$	$\cdots$	5935	$\cdots$	$\cdots$	$\cdots$	5813	$\cdots$	$\cdots$	$\cdots$	5612	$\cdots$	$\cdots$	$\cdots$
Ref. [22]	5796	6069	5946-6589	6054	5934	6164	$\cdots$	6183	5810	6043	$\cdots$	6065	5620	5914	6207	6233
Ref. [23]	$\cdots$	$\cdots$	$\cdots$	$\cdots$	5943	6223	$\cdots$	6225	5820	6100	$\cdots$	6089	$\cdots$	$\cdots$	$\cdots$	$\cdots$
Ref. [24]	5812	6077	6243	6285	5935	6201	6366	6216	$\cdots$	$\cdots$	$\cdots$	$\cdots$	$\cdots$	$\cdots$	$\cdots$	$\cdots$
Ref. [25]	5784	6048	6214	6226	5926	6190	6356	6203	$\cdots$	$\cdots$	$\cdots$	$\cdots$	$\cdots$	$\cdots$	$\cdots$	$\cdots$
Ref. [26]	5812	6077	6243	6258	5935	6201	6336	6216	5810	6108	6300	6123	5615	5913	6106	6121
Ref. [27][a]	5806	6079	6248	6271	5925	6198	6367	6220	5804	6108	6304	6131	5613	5918	6114	6137
Ref. [3]	5792	6100	6230	6270	5935	6220	6350	6250	5816	6097	6246	6135	5620	5912	6236	6273
Used	5792	6080	6245	6260	5935	6200	6360	6216	5813	6108	6300	6130	5612	5915	6100	6130

[a] Only the center values of three-quark predicted masses are listed.

$$\phi = \begin{pmatrix} \frac{1}{\sqrt{2}}\pi^0 + \frac{1}{\sqrt{6}}\eta & \pi^+ & K^+ \\ \pi^- & -\frac{1}{\sqrt{2}}\pi^0 + \frac{1}{\sqrt{6}}\eta & K^0 \\ K^- & \bar{K}^0 & -\sqrt{\frac{2}{3}}\eta \end{pmatrix}, \quad (20)$$

where $g_{\rm A}^q$ is the quark axial vector coupling constant that $g_{\rm A}^q = 1$ [32]; $f_{\rm m}$ is the pseudoscalar meson decay constant, and $f_\pi = 132$ MeV for pion.

The non-relativistic form of H_χ is:

$$H_\chi = \frac{\delta}{\sqrt{(2\pi)^3 2\omega_m}} \sum_{j=1}^{2} \frac{1}{f_{\rm m}} \left[\omega_{\rm m} \left(\frac{\boldsymbol{\sigma}\cdot\boldsymbol{p}_{\rm f}^j}{2m_{\rm f}} + \frac{\boldsymbol{\sigma}\cdot\boldsymbol{p}_{\rm i}^j}{2m_{\rm i}} \right) - \boldsymbol{\sigma}\cdot\boldsymbol{k} \right] \times \hat{I}_\chi^j \delta^3(\boldsymbol{p}_{\rm f}^j + \boldsymbol{k} - \boldsymbol{p}_{\rm i}^j), \quad (21)$$

where $\omega_{\rm m}$ and $\boldsymbol{k}$ are the energy and momentum of the pseudoscalar meson, respectively; $\boldsymbol{p}_{\rm i}^j$ and $\boldsymbol{p}_{\rm f}^j$ are the initial and final momentum of the jth light quark, respectively; $\hat{I}_\chi^j$ is the isospin operator acting on the jth light quark and written as:

$$\hat{I}_\chi^j = \begin{cases} a_u^\dagger a_d, & \text{for } \pi^-, \\ a_d^\dagger a_u, & \text{for } \pi^+, \\ \frac{1}{\sqrt{2}}(a_u^\dagger a_u - a_d^\dagger a_d), & \text{for } \pi^0, \end{cases} \quad (22)$$

where $a_q^\dagger$ and a_q are the creation and annihilation operators for the q quark, respectively.

In Eq. (21), a dimensionless parameter δ is introduced to take into account the uncertainties arising from the model [31]. In our previous work [3], f_π is taken as 93 MeV. This is equivalent to taking $\delta = \sqrt{2}$. Different values for δ can be found in the literature. They may be due to the different normalization conditions introduced to the interacting vertex [31].

With the wave functions and transition operators, the decay width can be expressed as:

$$\Gamma(A \to B + C) = 8\pi^2 \frac{|\boldsymbol{k}| E_{\rm B} E_{\rm C}}{M_{\rm A}} \frac{1}{2J_{\rm A}+1} \times \sum_{\rm spin} \left(|\mathcal{M}_{\rm PC}|^2 + |\mathcal{M}_{\rm PV}|^2 \right), \quad (23)$$

with the normalization convention

$$\langle B_f(\boldsymbol{P}_{\rm f}) | B_{\rm i}(\boldsymbol{P}_{\rm i}) \rangle = \delta^3(\boldsymbol{P}_{\rm f} - \boldsymbol{P}_{\rm i}). \quad (24)$$

$J_{\rm A}$ is the spin of the initial state.

Table 2. The ranges of the K for the bottom baryons. In Ref. [25], the value of α_ρ used in the calculation of the strong and electromagnetic decay is $\alpha_\rho = 403$ MeV, and the K is estimated with $\alpha_\rho^4 = 3Km_\rho$.

References	K (GeV^3)
Ref. [25]	≈ 0.024
Ref. [26]	0.02377 ± 0.00014
Ref. [27]	0.0254 ± 0.0012 or 0.0245 ± 0.0023

Numerical Results and Discussions

A. Parameters

Within the harmonic oscillator approximation, i.e., neglecting the hyperfine effects [17,18,33,34], there are two kinds of model parameters in the Hamiltonian that are the quark mass and the spring constant K. The masses of quarks are taken as $m_{\rm u} = m_{\rm d} = 0.3$ GeV, $m_{\rm s} = 0.5$ GeV, and $m_{\rm b} = 5$ GeV which are the same as our previous work [3].

The spring constant K is an essential parameter of the non-relativistic component quark model. Its value indicates the strengths of interactions between quarks. Both K and the mass of quarks determine the harmonic oscillator strengths, subsequently determining the root-mean-square radius of the hadrons, as shown in the Framework Section. Ideally, K is flavor-independent, however, for the phenomenological approach, K could take different values in different hadron systems. Usually, the value of K is extracted by fitting the spectrum of hadrons. For the bottom baryons, the values of K adopted in different works are listed in Table 2 as a comparison.

The wave function used in this work is the single Gauss function. Thus, the values of α_ρ and α_λ should contain the non-harmonic effects and may deviate from the values extracted from the hadron spectrum. Hence, α_ρ and α_λ should be treated as two independent parameters from the perspective of phenomenology. In this work, in order to avoid the uncertainty caused by the charmed hadrons or light hadrons, we only consider those decay processes that involve the bottom baryons to extract the values of these parameters. However, only the decay width of $\Xi_b^- \to \Lambda_b^0 \pi^-$ has been measured with which the parameters cannot be effectively restricted. As a result, the strong decays of the other bottom baryons, such as the $\Sigma_b^{(*)} \to \Lambda_b^0 \pi$ [35] strong decay processes, are introduced to constrain the parameters.

The strong decay vertices of $\Sigma_b \to \Lambda_b^0 \pi$ will appear in the hadronic weak decay pole terms that are not shown separately. Its transition amplitudes are calculated with the chiral quark model introduced in the Framework Section. Apparently, the available data for the strong decay width of $\Sigma_b^+ \to \Lambda_b^0 \pi^+$ and $\Xi_b^- \to \Lambda_b^0 \pi^-$ are insufficient to

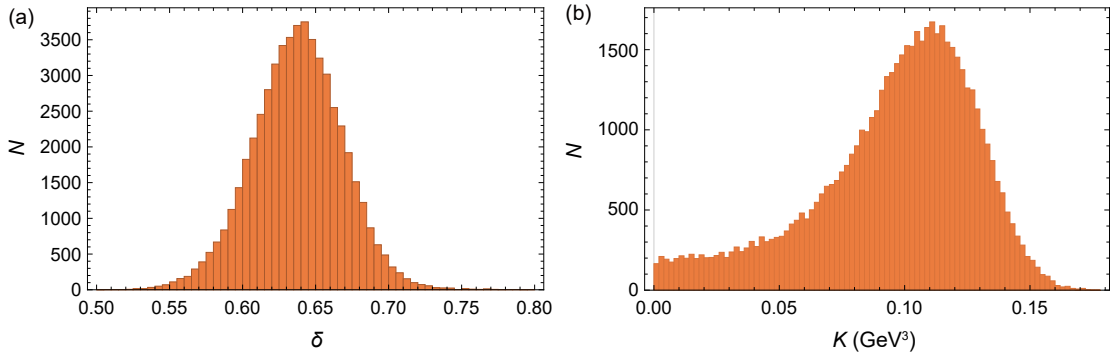

Fig. 5. The distributions of δ and K constrained by the strong decay channel $\Sigma_b^+ \to \Lambda_b^0\pi^+$ and the hadronic weak decay channel $\Xi_b^- \to \Lambda_b^0\pi^-$. The total number of the samples is about 54300.

Table 3. The amplitudes for each process (in unit of 10^{-9} GeV$^{-1/2}$). The spin of the initial and final baryon is taken as 1/2. "CS-I" and "CS-II" are used to label the first and second type of the CS processes, respectively. The symbol "–" indicates that the decay process is not dynamically allowed for the corresponding channel.

Processes	$\Xi_b^- \to \Lambda_b^0\pi^-$	$\Xi_b^0 \to \Lambda_b^0\pi^0$	$\Omega_b^- \to \Xi_b^0\pi^-$	$\Omega_b^- \to \Xi_b^-\pi^0$
DPE	−9.86	–	3.05	–
CS-I	8.65	6.12	–	–
CS-II	–	2.32	–	0.71
WS	–	0	–	–
SW($\Xi_b^0\|^2P_\rho$))	−21.37 − 0.09i	−14.91 − 0.06i	–	–
SW($\Xi_b^0\|^4P_\rho$))	−27.58 − 0.07i	−19.24 − 0.05i	–	–
Total	−50.16 − 0.16i	−25.70 − 0.11i	3.05	0.71

Table 4. The branching ratios (in %) of $\Xi_b \to \Lambda_b^0\pi$ and $\Omega_b \to \Xi_b\pi$ are compared with the experimental data and other models results. "⋯" means that the data are unavailable from the corresponding references. Our results are listed in the last line and the error is related with the uncertainties of δ and K.

References	$\Xi_b^- \to \Lambda_b^0\pi^-$	$\Xi_b^0 \to \Lambda_b^0\pi^0$	$\Omega_b^- \to \Xi_b^0\pi^-$	$\Omega_b^- \to \Xi_b^-\pi^0$
Experimental data	0.89 ± 0.32 [15]	⋯	⋯	⋯
Ref. [4]	0.42 ± 0.05	0.26 ± 0.03	$(6.5 \pm 0.7) \times 10^{-3}$	$(3.2 \pm 0.3) \times 10^{-4}$
Ref. [7]	2 – 8	1 – 4	⋯	⋯
Ref. [8]	0.19 – 0.76	0.09 – 0.37	$(1.1 - 4.3) \times 10^{-4}$	$(0.6 - 2.2) \times 10^{-4}$
Ref. [10]	0.8 ± 0.3	⋯	⋯	⋯
Ref. [12]	0.63 ± 0.42	0.32 ± 0.21	⋯	⋯
Previous work [3]	0.14 ± 0.073	0.017 ± 0.015	⋯	⋯
This work	0.92 ± 0.40	0.22 ± 0.13	$(9.12 \pm 0.07) \times 10^{-3}$	$(4.77 \pm 0.035) \times 10^{-4}$

determine the parameters α_ρ, α_λ, and δ. Therefor, we have to reconsider the relation given by Eq. (13) to reduce the parameters, and treat δ and K as the free parameters to be determined in our framework.

The center values and the errors of these two parameters are extracted with Monte Carlo (MC) technique instead of fitting. The acceptance-rejection method [35] is used to generate samples of δ and K. We assume that the distribution of the decay width of $\Sigma_b^+ \to \Lambda_b^0\pi^+$ and $\Xi_b^- \to \Lambda_b^0\pi^-$ obeys the normal distribution. The sampling interval of δ is $(0.5, 0.8)$ and the one of K is $(0, 0.18)$ GeV^3.

The distributions of the parameters δ and K constrained by the strong decay of $\Sigma_b^+ \to \Lambda_b^0\pi^+$ and the hadronic weak decay of $\Xi_b^- \to \Lambda_b^0\pi^-$ are shown in Fig. 5. The total number of the samples is about 5.4×10^4 for each parameter. Figure 5(a) clearly shows that the distribution of δ obeys the normal distribution. The center value of δ is about 0.64 that is slightly larger than the value used in Ref. [31]. The standard deviation is about 0.03. As shown in Fig. 5(b), the distribution of K apparently deviates from the normal distribution. It may result from the lack of the input data. We take the maximum probability value that is about 0.11 GeV^3 as the center value of K and take the half-width of the distribution that is about 0.02 GeV^3 as the error of K. It should be noted that the center value of K extracted in this work is significantly larger than the values listed in Table 2. In contrast, the corresponding α_ρ of Ξ_b is about 0.57 GeV that is about 1.4 times α_ρ (0.40 GeV) used in Ref. [25]. This deviation can be ascribed to the approximation of the spatial wave function as mentioned before. As discussed earlier, the deviation of α_ρ is acceptable.

B. The Numerical Results and Discussions

With the center values of δ, K and the quark masses determined in the previous section, we calculate the amplitudes for each channel and the non-zero transition matrix elements are listed in Table 3. Depending on the distribution of δ and K, the center values and the errors of the calculated branching ratios of $\Xi_b \to \Lambda_b^0\pi$ and $\Omega_b \to \Xi_b\pi$ are listed in Table 4.

The Asymmetry Parameter. For these hadronic weak decay channels $\Xi_b \to \Lambda_b^0\pi$ and $\Omega_b \to \Xi_b\pi$, the b quark does not participate in the interactions and behaves as a spectator. One would expect that the heavy quark spin symmetry (HQSS) should hold in these decay channels. As a consequence, one can describe the decay processes through the transitions between the light quarks, i.e., $s_i^P \to s_{f_1}^{P_1} s_{f_2}^{P_2}$ with s_i ($s_{f_{1,2}}$) and P ($P_{1,2}$) denoting the spin and parity of the initial (final) light quarks (or quark-antiquark), respectively. With this convention, the

hadronic weak decay of $\Xi_b \to \Lambda_b^0\pi$ with the light flavor of anti-triplet will be via $0^+ \to 0^+0^-$. It shows that only the S-wave transition operator can conserve the angular momentum. Thus, the leading order amplitude should be given by the S-wave PV transition. Similarly, the decay of $\Omega_b \to \Xi_b\pi$ with the light flavor of sextet will be via $1^+ \to 0^+0^-$, and the leading order amplitude will be given by the P-wave PC transition.

The numerical results do show that the contributions of the PC operators to the process of $\Xi_b \to \Lambda_b^0\pi$ and the contributions of the PV operators to the process of $\Omega_b \to \Xi_b\pi$ vanish as we expected. This causes that the asymmetry parameter α [35], which is determined by the interference between the PC and PV components of the transition amplitude

$$\alpha = \frac{2\mathrm{Re}\left[\mathcal{M}_{\mathrm{PV}}^{*}\mathcal{M}_{\mathrm{PC}}\right]}{|\mathcal{M}_{\mathrm{PC}}|^2 + |\mathcal{M}_{\mathrm{PV}}|^2}\,, \tag{25}$$

vanishes for both $\Xi_b \to \Lambda_b^0\pi$ and $\Omega_b \to \Xi_b\pi$. This vanishing asymmetry parameter is crucial for testing the heavy quark symmetry in these two processes.

$\Xi_b \to \Lambda_b^0\pi$. Figures 1 and 2 clearly reveal that the $\Xi_b^- \to \Lambda_b^0\pi^-$ and $\Xi_b^0 \to \Lambda_b^0\pi^0$ decay processes are not exactly the same. In the following, we will compare the contributions of the DPE processes, CS processes, and the pole terms to reveal the role played by flavor symmetry and hadronic weak decay mechanisms for these two processes.

Due to the suppression of the neutral current interaction, we do not consider the DPE in $\Xi_b^0 \to \Lambda_b^0\pi^0$. The CS-I process can contribute to both the $\Xi_b^- \to \Lambda_b^0\pi^-$ and $\Xi_b^0 \to \Lambda_b^0\pi^0$ processes. Comparing the calculated amplitudes from the CS-I process in Table 3, one can find that the ratio of about 1.4 between these two channels satisfies the isospin symmetry. The weak transition operator of the CS-I process is $s \to u\bar{u}d$, and according to the weak isospin analysis, we have

$$\frac{\mathcal{A}_{\mathrm{CS-I}}(\Xi_b^- \to \Lambda_b^0\pi^-)}{\mathcal{A}_{\mathrm{CS-I}}(\Xi_b^0 \to \Lambda_b^0\pi^0)} = \frac{\langle 1,-1|\frac{1}{2},-\frac{1}{2};\frac{1}{2},-\frac{1}{2}\rangle}{\langle 1,0|\frac{1}{2},\frac{1}{2};\frac{1}{2},-\frac{1}{2}\rangle} = \sqrt{2}. \tag{26}$$

This result can also be obtained from the transition diagrams directly. One can see that figures 1(b) and 2(a) share the same decay mechanism of the CS-I transition. In Fig. 2(a), the projection of the $u\bar{u}$ component to the π^0 wave function will contribute a factor of $1/\sqrt{2}$.

The CS-II process only contributes to the decay of $\Xi_b^0 \to \Lambda_b^0\pi^0$. The amplitude of the CS-II process is smaller compared with the CS-I process, as shown in Table 3. It is because of the difference arising from the convolution of the spatial wave functions.

As shown in Table 3, we see that most of the states listed in Table 1 have no contributions to the pole terms. Figure 1 illustrates that the WS process does not contribute to the decay channel $\Xi_b^- \to \Lambda_b^0\pi^-$. In contrast, there are two WS transition processes contributing to the decay $\Xi_b^0 \to \Lambda_b^0\pi^0$, as depicted in Figs. 2(c) and 2(d). Nevertheless, the contributions of these two processes cancel each other out, since the signs of the $u\bar{u}$ and $d\bar{d}$, and the flavor components of the π^0 flavor wave function, are opposite. On the other hand, only the two states, $\Xi_b^0(|^2P_\rho\rangle)$ and $\Xi_b^0(|^4P_\rho\rangle)$, contribute to the SW pole terms. It indicates that the transitions between the bottom baryons are subjected to strict restrictions because of the HQSS as mentioned before or the selection rules determined by the symmetry. Taking the contribution of $\Xi_b^0(^2P_\lambda)$ as an example, the spin wave functions of the light quark pairs in both Ξ_b and $\Xi_b(^2P_\lambda)$ are spin-singlet. However, the spin operator contained in H_χ corresponds to spin doublet. According to the Wigner−Eckart theorem, the values of the spin transition matrix element must be 0. Consequently, the strong transition $\Xi_b \to \Xi_b(^2P_\lambda)\pi$ is forbidden. More detailed discussions can be found in Ref. [3].

The ratio between the amplitudes of the SW pole terms for $\Xi_b^- \to \Lambda_b^0\pi^-$ and $\Xi_b^0 \to \Lambda_b^0\pi^0$ is also about 1.4, which is given by the isospin factors for the π^- and π^0 productions at the strong interaction vertices. It can be recognized from Fig. 1(c) and Fig. 2(e) which share the same transition mechanism except that the $u\bar{u}$ component will project to the π^0 flavor wave function and contribute a factor of $1/\sqrt{2}$.

Notice that the amplitudes of the SW pole terms are much larger than those of the DPE and CS processes in both $\Xi_b^- \to \Lambda_b^0\pi^-$ and $\Xi_b^0 \to \Lambda_b^0\pi^0$. It suggests that the pole terms should play a crucial role in understanding the decay properties of these two processes. With the interference effects among all the amplitudes taken into account, the ratio of about 2 between their total amplitudes does deviate from $\sqrt{2}$ (or numerically 1.4) given by the isospin factor. It results in that the branching ratio fraction between the $\Xi_b^- \to \Lambda_b^0\pi^-$ and $\Xi_b^0 \to \Lambda_b^0\pi^0$ is about 4. In contrast, if we neglect the contributions of the factorizable process, i.e., the DPE contribution to $\Xi_b^- \to \Lambda_b^0\pi^-$, we will have

$$\mathrm{Br}(\Xi_b^- \to \Lambda_b^0\pi^-) \approx 2\mathrm{Br}(\Xi_b^0 \to \Lambda_b^0\pi^0)\,, \tag{27}$$

which is close to the prediction of Ref. [4], i.e., $\mathrm{Br}(\Xi_b^- \to \Lambda_b^0\pi^-) \approx 1.62\times\ \mathrm{Br}(\Xi_b^0 \to \Lambda_b^0\pi^0)$ and is the same as the results of Refs. [7,8,12].

From the perspective presented in Refs. [4,5,11,13], the emitted pion of HFC decays is truly soft and the S-wave amplitude is evaluated with current algebra in the soft-meson limit. The PV amplitude can be expressed as [19]:

$$A^{\mathrm{com}} = -\frac{\sqrt{2}}{f_\pi}\langle \mathcal{B}_f|[Q_5^a, H_{\mathrm{W}}^{\mathrm{pv}}]|\mathcal{B}_i\rangle + \lim_{q^\mu\to 0} q^\mu R_\mu, \tag{28}$$

where Q_5^a is the axial charge and defined as follows:

$$Q_5^a = \int \mathrm{d}x^3 \bar{q}\gamma^0\gamma^5\frac{\lambda^a}{2}q. \tag{29}$$

The second term in Eq. (28) vanishes if R_μ is a smooth function with $q^\mu \to 0$. The implementation of the soft pion theorem requires satisfaction of this condition. Alternatively, if there exists a singularity as $q^\mu \to 0$, contributions from the second term in Eq. (28) cannot be neglected. In the hadronic weak decays considered here, such a singularity can occur due to the presence of the intermediate states (propagators) of which the pole positions can be "degenerate" with the initial or final baryon states. Such a situation can be recognized by inserting a complete set of intermediate states in the time-ordered product in R_μ. Then, the R_μ term will be enhanced given that one intermediate state has a mass close to the mass of $|\mathcal{B}_i\rangle$ in the WS transition or of $|\mathcal{B}_f\rangle$ in the SW transition. This also makes a difference between our approach and those [4,5,11,13] which only include the first term in Eq. (28).

In Refs. [4,7,8,10], the S-wave amplitudes are also expressed with the current algebra technique, but the hadron matrix elements are calculated in different ways. Thus, different results are obtained. In Ref. [12], the S-wave amplitude of $\Xi_b^- \to \Lambda_b^0\pi^-$ is related to the S-wave nonleptonic decays of Λ, Σ, and Ξ, and the branching fraction of $\Xi_b^0 \to \Lambda_b^0\pi^0$ is expected to be half of $\Xi_b^- \to \Lambda_b^0\pi^-$. However, the contribution of the DPE and the CS processes and the interference of all the processes are not further discussed in these works.

Our previous result for the branching ratio is $(0.14 \pm 0.073)\%$ for $\Xi_b^- \to \Lambda_b^0\pi$ [3], which is also much smaller than the experimental data. There, the value of $K = 0.035\ \mathrm{GeV}^3$ is adopted based on the values extracted from the heavy baryon spectra and is much smaller than the value used in this work. As pointed out in Ref. [3] the amplitude is sensitive to the value of K and can be different for hadrons with different flavors. In this work, instead, the value of K is constrained by the experimental data for $\Xi_b^- \to \Lambda_b^0\pi^-$, with which one can predict the branching ratios of other channels. Because of this, the branching ratio of $\Xi_b^0 \to \Lambda_b^0\pi^0$ obtained in this work is different from the previous work [3], but should be more self-consistent here.

$\Omega_b \to \Xi_b\pi$. For the decay process of $\Omega_b^- \to \Xi_b^0\pi^-$, the tree-level transition is via the DPE process as shown in Fig. 3, and for $\Omega_b^- \to \Xi_b^-\pi^0$, the tree-level transition is via the CS-II process as shown in Fig. 4. It should be noted that no pole terms can contribute to these two processes. It explains that the error of $\mathrm{Br}(\Omega_b \to \Xi_b\pi)$ is much smaller than that of Ξ_b. Meanwhile, two interesting features arise from the decay of $\Omega_b^- \to \Xi_b^0\pi^-$ and $\Xi_b^-\pi^0$. Firstly, these two transitions cannot be related to each other directly via isospin symmetry. Due to the effects of color suppression, the branching ratio of $\Omega_b^- \to \Xi_b^-\pi^0$ is

supposed to be much smaller than that of $\Omega_b^- \to \Xi_b^0\pi^-$ by about one order of magnitude which is consistent with the prediction given by Ref. [4]. Secondly, the branching ratios of $\Omega_b \to \Xi_b\pi$ are much smaller than those of $\Xi_b \to \Lambda_b^0\pi$ as shown in Table 4, which is because of the absence of the pole terms. More specifically, this is because $\Omega_b^- \to \Xi_b^0\pi^-$ proceeds only through the DPE process that is proportional to the momentum of the final state which is about 205 MeV. It leads to the suppression of the DPE amplitude which is consistent with the conclusion of Ref. [4]. In addition, as clearly shown in Table 3, the amplitude of the DPE process of $\Omega_b^- \to \Xi_b^0\pi^-$ and the CS-II amplitude of $\Omega_b^- \to \Xi_b^-\pi^0$ are much smaller than that of the pole terms of $\Xi_b \to \Lambda_b^0\pi$. Thus, the decay width of $\Omega_b^- \to \Xi_b^-\pi^0$ is about two orders of magnitude smaller than that of $\Xi_b^- \to \Lambda_b^0\pi^-$ although the phase space of $\Omega_b \to \Xi_b\pi$ is relatively larger.

Before the conclusion, we would like to discuss the final-state interaction in bottom baryon decays. The role played by the final-states interaction has aroused much concern about the branching ratio anomaly and CP violation effects in hadronic weak decay of heavy baryons [36−40]. It is generally accepted that the final-state interaction plays an essential role in the study of exotic states near threshold [41−43]. As we have learned in many cases (also see Refs. [41−43] and the references therein), the final-state interaction can become important when the interaction is an S-wave and near threshold. At leading order, only the P-wave contributes to the final state interaction of $\mathcal{B}_f\pi$ to ensure the P-parity conservation. This leads to the final-state interaction being less important since the HFC hadronic weak decay is a near-threshold process. So, the effects of the final-state interaction are neglected at this moment.

Summary and Outlook

The HFC hadronic weak decays of $\Xi_b \to \Lambda_b^0\pi$ and $\Omega_b \to \Xi_b\pi$ are investigated in the framework of the NRCQM. In our calculation, the values of the quark masses are consistent with the commonly adopted values. The values of the spring constant K and the dimensionless parameter δ are extracted from the measured decay widths of $\Xi_b^- \to \Lambda_b^0\pi^-$ and $\Sigma_b^+ \to \Lambda_b^0\pi^+$. The value of K extracted in this work is different from that given by the hadron spectrum study. This may result from the harmonic oscillator approximation, which is an oversimplified approach in our framework. Since the systematic model uncertainties can be absorbed into some of the model parameters, the advantage of the NRCQM framework is to treat the DPE processes, CS processes and pole terms in a self-consistent way, and their relative strengths can be reliably evaluated.

With the contributions of the DPE processes, CS processes and pole terms systematically considered, the numerical results show that these mechanisms manifest themselves differently and are crucial for understanding the branching ratio fraction between $\Xi_b^- \to \Lambda_b^0\pi^-$ and $\Sigma_b^+ \to \Lambda_b^0\pi^+$. It shows that the contributions of the pole terms can be significantly larger than the contributions of the DPE and CS processes. This is analogous to the case of the $\Xi_c \to \Lambda_c\pi$. Our analysis also shows that the decay width of $\Omega_b \to \Xi_b\pi$ is significantly smaller than that of $\Xi_b \to \Lambda_b^0\pi$ due to the absence of the pole terms. The prediction can be examined by the future experiments at LHCb and Belle-II.

Acknowledgments

This work was supported in part by the National Natural Science Foundation of China (Grant Nos. 12505110, 12235018, 12547105, and 12375073).

References

[1] Aaij R, Abellán Beteta C, Ackernley T *et al.* (LHCb Collaboration) 2020 *Phys. Rev. D* **102** 071101
[2] Voloshin M B 2000 *Phys. Lett. B* **476** 297
[3] Niu P Y, Wang Q, and Zhao Q 2022 *Phys. Lett. B* **826** 136916
[4] Cheng H Y, Liu C W, and Xu F R 2022 *Phys. Rev. D* **106** 093005
[5] Cheng H Y, Cheung C Y, Lin G L, Lin Y C, Yan Y M, and Yu H L 1992 *Phys. Rev. D* **46** 5060
[6] Sinha S and Khanna M P 1999 *Mod. Phys. Lett. A* **14** 651
[7] Li X and Voloshin M B 2014 *Phys. Rev. D* **90** 033016
[8] Faller S and Mannel T 2015 *Phys. Lett. B* **750** 653
[9] Gronau M and Rosner J L 2016 *Phys. Lett. B* **757** 330
[10] Voloshin M B 2019 *Phys. Rev. D* **100** 114030
[11] Cheng H Y, Cheung C Y, Lin G L, Lin Y C, Yan T M, and Yu H L 2016 *JHEP* **03** 028
[12] Gronau M and Rosner J L 2016 *Phys. Rev. D* **93** 034020
[13] Cheng H Y and Xu F R 2022 *Phys. Rev. D* **105** 094011
[14] Aaij R, Abellán Beteta C, Adeva B *et al.* (LHCb Collaboration) 2015 *Phys. Rev. Lett.* **115** 241801
[15] Aaij R, Abdelmotteleb A S W, Abellan Beteta C *et al.* (LHCb Collaboration) 2023 *Phys. Rev. D* **108** 072002
[16] Aaij R, Abellán Beteta C, Adeva B *et al.* (LHCb Collaboration) 2019 *Phys. Rev. D* **99** 052006
[17] Yaouanc A Le, Oliver L, Pene O, and Raynal J C 1988 *Hadron Transitions in the Quark Model* (Gordon and Breach Science Publishers)
[18] Isgur N and Karl G 1978 *Phys. Rev. D* **18** 4187
[19] Yaouanc A Le, Pene O, Raynal J C, and Oliver L 1979 *Nucl. Phys. B* **149** 321
[20] Buchalla G, Buras A J, and Lautenbacher M E 1996 *Rev. Mod. Phys.* **68** 1125
[21] Workman R L, Burkert V D, Crede V *et al.* (Particle Data Group Collaboration) 2022 *PTEP* **2022** 083C01
[22] Kim Y, Oka M, and Suzuki K 2025 *Phys. Rev. D* **111** 034014
[23] Li Z Y, Yu G L, Wang Z G, and Gu J Z 2024 *Eur. Phys. J. C* **84** 1310
[24] Bijker R and Ortiz-Pacheco E 2024 *Nuovo Cim. C* **47** 175
[25] Bijker R, García-Tecocoatzi H, Giachino A, Ortiz-Pacheco E, and Santopinto E 2022 *Phys. Rev. D* **105** 074029
[26] Ortiz-Pacheco E and Bijker R 2023 *Phys. Rev. D* **108** 054014
[27] García-Tecocoatzi H, Giachino A, Ramirez-Morales A, Rivero-Acosta A, Santopinto E, and Vaquera-Araujo C A 2024 *Phys. Rev. D* **110** 114005
[28] Manohar A and Georgi H 1984 *Nucl. Phys. B* **234** 189
[29] Li Z P, Ye H X, and Lu M H 1997 *Phys. Rev. C* **56** 1099
[30] Zhao Q, Al-Khalili J S, Li Z P, and Workman R L 2002 *Phys. Rev. C* **65** 065204
[31] Zhong X H and Zhao Q 2008 *Phys. Rev. D* **77** 074008
[32] Arifi A J, Suenaga D, and Hosaka A 2021 *Phys. Rev. D* **103** 094003
[33] Isgur N and Karl G 1977 *Phys. Lett. B* **72** 109
[34] Yoshida Y, Hiyama E, Hosaka A, Oka M, and Sadato K 2015 *Phys. Rev. D* **92** 114029
[35] Navas S, Amsler C, Gutsche T *et al.* (Particle Data Group Collaboration) 2024 *Phys. Rev. D* **110** 030001
[36] Han J J, Jiang H Y, Liu W, Xiao Z J, and Yu F S 2021 *Chin. Phys. C* **45** 053105
[37] Jia C P, Jiang H Y, Wang J P, and Yu F S 2024 *JHEP* **11** 072
[38] Duan Z D, Wang J P, Li R H, Lü C D, and Yu F S 2025 *JHEP* **09** 160
[39] Hu X H, Jia C P, Xing Y, and Yu F S 2025 *Phys. Rev. D* **111** 076002
[40] Cheng H Y, Xu F R, and Zhong H 2025 *Phys. Rev. D* **112** 054022
[41] Guo F K, Hanhart C, Meißner U G, Wang Q, Zhao Q, and Zou B S 2018 *Rev. Mod. Phys.* **90** 015004
[42] Guo F K, Liu X H, and Sakai S 2020 *Prog. Part. Nucl. Phys.* **112** 103757
[43] Dong X K, Guo F K, and Zou B S 2021 *Phys. Rev. Lett.* **126** 152001